

Effect of Rotatory Arc Welding Technology on Metallurgical and Mechanical Performance of Armour Grade Steel Joints

DOI : 10.22486/iwj.v55i2.212411

¹N. Sankar, ²S. Malarvizhi, ³V. Balasubramanian,
⁴A. Hafeezur Rahman and ⁵V. Balaguru

¹Research Scholar, ²Professor, ³Professor, Head and Director,
⁴Scientist – F, ⁵Outstanding Scientist

^{*,1,2,3}Centre for Materials Joining and Research (CEMAJOR)

Department of Manufacturing Engineering, Annamalai University, Annamalainagar

^{4,5}Combat Vehicles Research & Development Establishment (CVRDE)

DRDO, Avadi, Chennai

*Email: jeejoo@rediffmail.com

ORCID : N. Sankar : <https://orcid.org/0000-0001-5840-9990>

ORCID : S. Malarvizhi: <https://orcid.org/0000-0003-3934-3409>

ORCID : V. Balasubramanian : <https://orcid.org/0000-0002-4254-3674>



Abstract

This work is aimed to investigate the arc rotation effect on mechanical properties and metallurgical characteristics of 18 mm thickness armour grade quenched and tempered (Q & T) steel joints. Mechanical properties like tensile, impact toughness and microhardness were evaluated from welded joints. Metallurgical characteristics of welded joints like macrostructure, microstructure, and weld metal chemical composition were analyzed. From the results, it is observed that the rotating arc gas metal welded (RTA-GMW) joint contain minimum heat affected zone width (1.8 mm) and exhibits better tensile properties (784 MPa) due to the decrease in heat density caused by arc rotation of the joining process. The impact toughness properties of weld joint showed 36 % improvement than the unwelded base metal. Microstructural studies also revealed higher volume percentage of fine delta ferrite (δ -Fe) with vermicular type δ -Fe morphological feature in the weld joint. The rotation arc caused reduction in heat input, enhanced strength, impact toughness properties and creation of vermicular type δ -Fe morphology in armour grade Q&T steel welded joints.

Key words: Armour steel, rotating arc welding, mechanical properties, metallurgical behaviour.

1.0 Introduction

Conducive to meet better ballistic requirement and weldability, the high strength armour grade steels were developed. Armour steels have enhanced mechanical properties and ballistic performance to meet the requirements of military vehicles. Armour grade steels achieved superior mechanical properties (toughness and strength) by quenching and tempering (Q&T) processes [1]. Now days the armour grade steels are welded by many fusion welding processes [2]. However, drop in toughness and strength was recorded after welding because of high density thermal cycles [3]. In general, the higher heat density leads to wider heat affected zone (HAZ) width and

elongated coarse particles in the weld metal region. This effects in reduction in mechanical strength and ballistic performance of these welded joints [4]. Therefore, to reduce heat density and improve weld joint mechanical properties, suitable welding technique is need of the hour. The new emerging "spin arc" (or) "rotating arc" welding technique fulfills the above requirements. In rotating arc technique, the wire will rotate in circular motion among the two plates to be welded [5]. The rotation arc generates centrifugal force which acts on the molten pool and minimizes heat density and HAZ width. Another important advantage of this technique is, no need of edge preparation for welding of higher thickness steel plates [6]. Being a narrower gap welding method, additional

joint configuration is not necessary for the process. In such wise, machining time (edge preparation) reduces greatly, and thus overall productivity will increase. Sugitani et al. [7] designed and developed automatic higher-speed rotating technique for joints of steel plate with high thickness. Wenhong et al. [8] examined the effect of side wall penetration on arc rotating narrower gap GMA welding process. Linga raju et al. [9] examined the influence of arc rotation on weld bead geometry. The authors pointed that arc rotation in GMAW is found to increase the weld bead geometry. Vengatesh et al. [10] compared the metallurgical and tensile, impact toughness properties of carbon steel joints with conventional GMAW and spin arc GMAW process. The authors noted that the spin arc GMAW welding process improved the joint quality and productivity. Recently, Abo Al Ela et al. [11] the influence of SMAW settings on the structural qualities of armour steel welded joints was investigated. According to the authors, excessive heat input and insufficient preheating temperatures degrade mechanical characteristics and generate an undesirable microstructure in the weld metal areas. Ambuj Saxena et al. [12] performed SMAW using austenitic stainless steel and low hydrogen ferritic steel electrodes for welding of armour grade steels. Results revealed that using ASS electrode give good impact toughness than LHF electrode. Mohsen Amraeia et al. [13] explored the influence of heat inputs of ultra-high strength steel joints. According to the findings of that study, when heat input increases, mechanical strength of

joint decreases due to the creation of coarser delta ferrite microstructures in the welded metal regions. The impact of various joint configurations on the mechanical properties of 15 mm thick Q & T steel weld joints was studied. According to the authors, a weld junction with a double "V" butt joint has greater robustness than other groove designs [14]. Ding min et al. [15] have studied the mechanical strength of Q & T steel joints by spin arc GMAW welding process. The authors reported, the spin arc GMAW joints showed satisfied mechanical properties. Based on the above literature reviews, it is clearly that only a few studies on rotating arc welding of steel plates have been described softer. However, there is no research work on welding armour grade steel plates by the rotating arc welding method. Hence, the current research work focuses on the effect of rotating arc gas metal arc welding on mechanical properties and metallurgical behaviour of armour grade Q and T steel weld joints.

2. Experimental Details

The base metal for this experiment was 18 mm thick rolled homogenized armour (RHA) steel. The quenching and tempering (Q and T) heat treatment techniques were used to create this steel. The base metal is primarily comprised of quenched and tempered martensite microstructures, as illustrated in **Fig. 1**. To deposit weld metal, an austenite stainless steel (ER307) filler wire with a diameter of 1.2 mm was employed in this work. The chemical composition (wt. %)

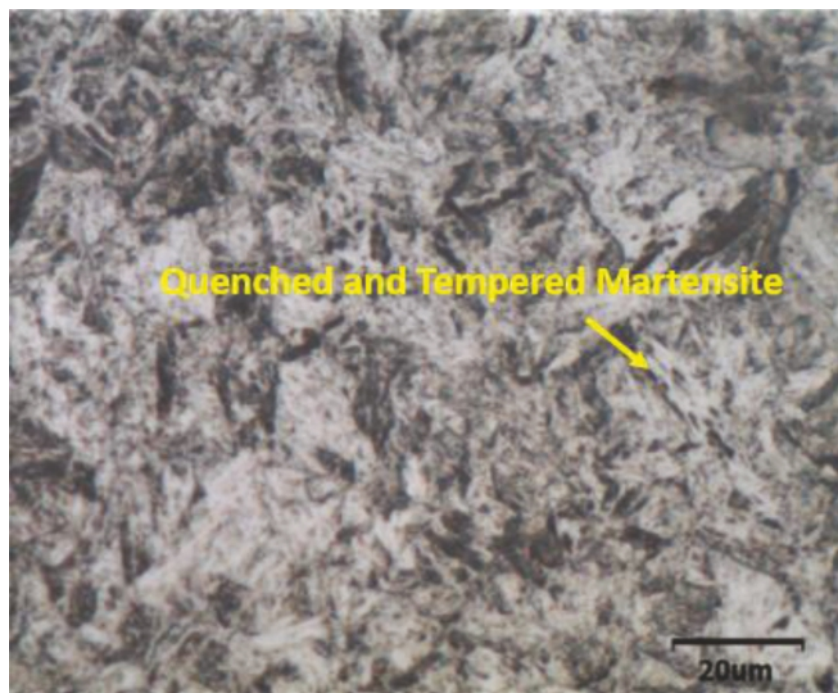


Fig. 1: Optical microstructure of base metal

and mechanical properties of base metal (BM) and filler metal (FM) are listed in **Tables 1** and **2**. Welding plates were machined along the rolling path and divided to 300x150x18 mm dimensions. The square butt joint was prepared without the "V" groove design. **Fig. 2** shows the top and side views of a weld joint configuration. Welding experiments were conducted out using semi-automatic GMAW equipment coupled with a rotating arc welding torch and the multi pass approach. **Fig. 3** shows the rotatory arc GMAW setup. **Table 3** shows the optimum welding process parameters used to manufacture the joints, as well as the heat input from the machine during each pass. After the joined plates were sliced and then machined to

the samples necessary dimensions. **Fig. 4** and **Fig. 5** demonstrate the pattern of specimen extraction from the welded joint as well as the specimen dimensions. The transverse tensile test was completed by universal testing machine with an electromechanical control capacity of 100 kN and test was conducted accordance with ASTM E8-14 guidelines [17]. Charpy impact testing (pendulum-type) machine was used to perform the Charpy impact toughness test. Three specimens were evaluated at each condition, and the averages of three samples were utilized to compute tensile and impact toughness properties. Vickers microhardness testing method was utilized to measure the microhardness

Table 1 : Chemical composition (wt %) of base metal (BM) and filler metal (FM)

Material	C	Si	Mn	P	S	Cr	Mo	Ni	Fe
BM	0.28	0.194	0.57	0.007	0.002	1.41	0.402	1.62	Bal
FM	0.06	0.56	1.20	0.024	0.012	20.89	2.38	9.02	Bal

Table 2 : Mechanical properties of base metal (BM) and filler metal (FM)

Material	Yield tensile strength (MPa) at 0.2% strain	Ultimate tensile strength (MPa)	Elongation (%) at 50 mm GL	Impact toughness @ RT (J)	Vickers hardness at 0.5 kg load (Hv)
BM	1200	1290	22	49	460
FM	680	740	26	66	250

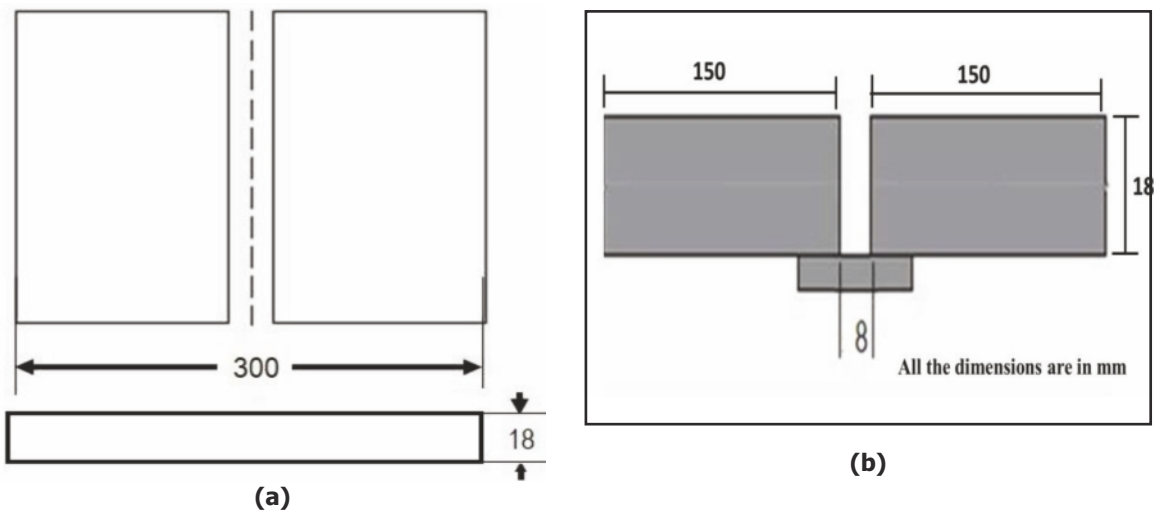


Fig. 2 : Configuration of weld joint (a) Top view, (b) Side view

Table 3 : Optimized Rotating Arc GMAW parameters used to fabricate the joints

Parameters	Unit	Weld Pass		
		1	2	3
Welding current	A	126	128	125
Arc voltage	V	22	23	23
Welding speed	mm/min	240	240	240
Wire feed rate	mm/min	180	180	180
Filler wire diameter	mm	1.2		
Arc rotational speed	rpm	1500		
Arc rotating diameter	mm	3		
Root gap	mm	8		
CTWD	mm	20		
Gas flow rate	lit/min	18		
Heat input	kJ/mm	0.69	0.73	0.71
		Cumulative Heat input		2.10



Fig. 3 : Rotating arc GMAW machine set up

throughout WM and HAZ regions. Microstructural studies of the weldments were performed using a light optical microscope (OM) in accordance with the ASTM E407-15 standard [18]. The microstructure of weld metal was revealed by etching the cross sectional weld surfaces with vilellas chemical. Heat-affected zone areas were etched with 2 percent nital reagent to disclose the WM and HAZ interface (IF) region.

3. Results

3.1 Mechanical properties

Table 4 shows the tensile characteristics of BM and RTA- GMW joint. Through the tensile test, the joints failed in the WM region. **Fig. 6** shows photographs of smooth tensile specimens. During tensile testing, the stress vs strain curves

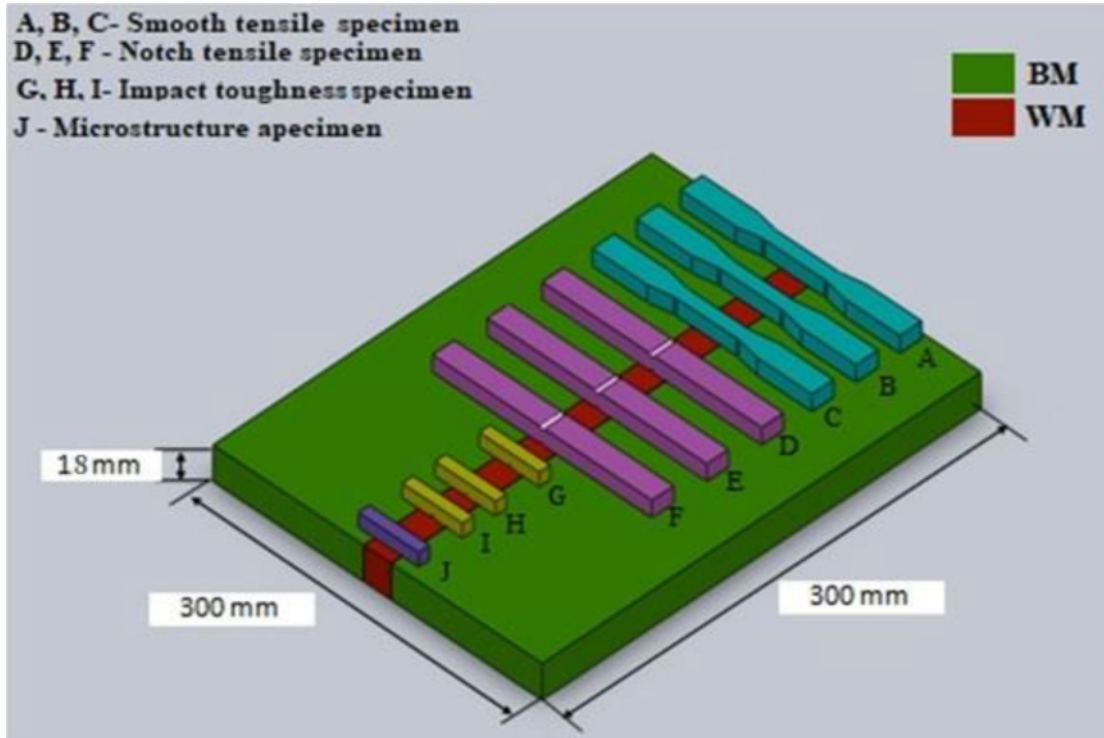


Fig. 4 : Scheme of extraction of specimens from the weld joint

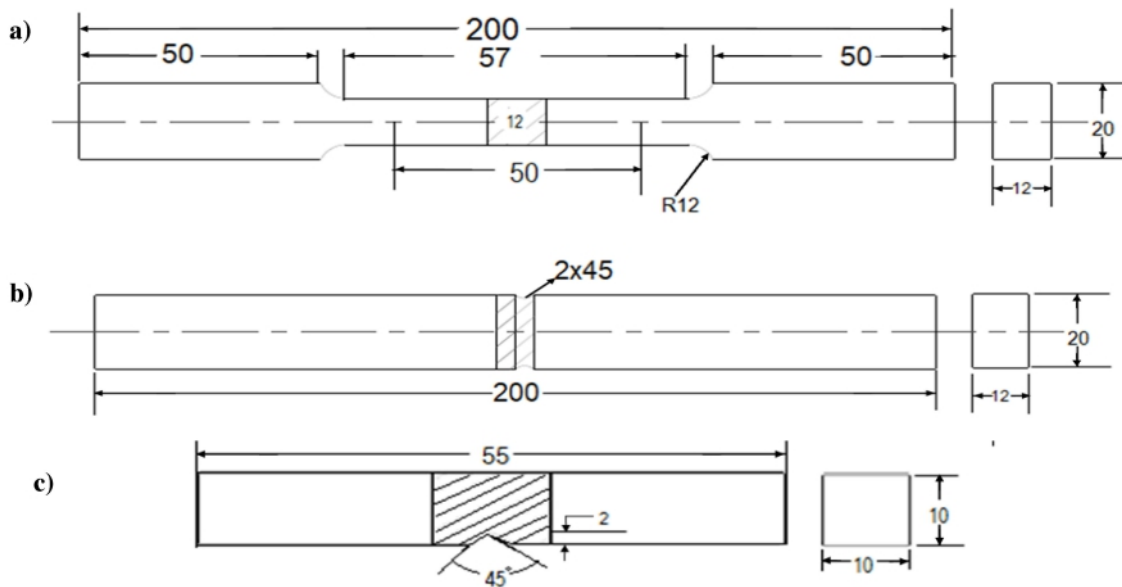


Fig. 5 : Dimensions of the specimens
 a) Smooth tensile specimen, b) Notch tensile specimen, c) Impact toughness specimen

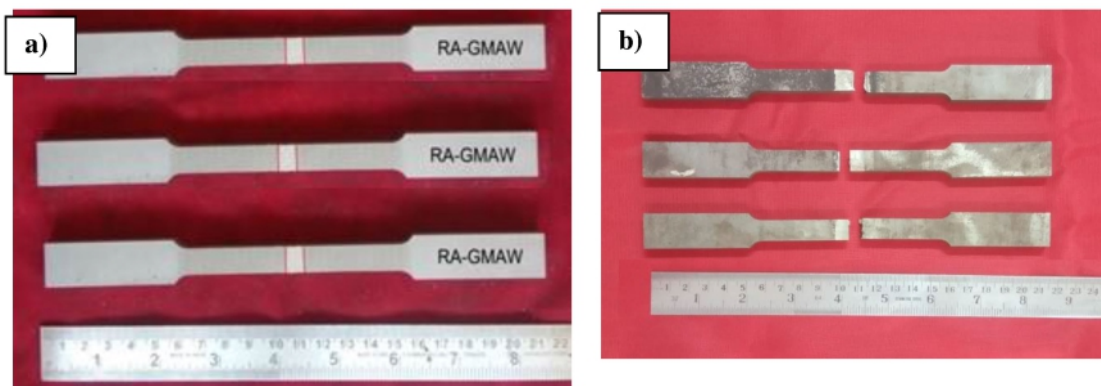
were recorded and as shown in **Fig. 7**. Ultimate tensile and yield strength of the BM were determined to be 1290 MPa and 1200 MPa, respectively. The ultimate tensile and yield strength of the RTA-GMW joint was 784 MPa and 665 MPa, respectively. The elongation of BM and RTA-GMW joints is 21 % and 24 %, respectively. It shows a 9 % increase in elongation of the welded joint when compared to BM.

The notch tensile strength of the RTA-GMW joint is 895 MPa and the NSR is more than one (>1) for the joint. This shows

that the BM and WM are unaffected by notches and hence fall within the "notch ductile" material group. **Table 4** shows the results of the joint efficiency value. According to the findings, the RTA-GMW joint has a joint efficiency of 62 %. **Table 4** shows the impact toughness results of BM and welded joints, and **Fig. 8** shows pictures of test samples. According to the findings, the RTA-GMW joint has a higher impact toughness than the BM joint. The impact toughness values of the RTA-GMW joint was 36 % higher than that of the BM joint.

Table 4 : Transverse tensile properties of welded joints

0.2% Yield strength (MPa)	Ultimate tensile strength (MPa)	Elongation in 50mm gauge length (%)	Notch tensile strength (MPa)	Notch strength ratio (NSR)	Joint Efficiency (%)	Failure location	Impact toughness @ RT (J)
665	784	24	895	1.10	62	WM	82



(a) Unnotched Tensile Specimen (before Testing)

(b) Unnotched Tensile Specimen (after Testing)

Fig. 6 : Photographs of tensile test specimen

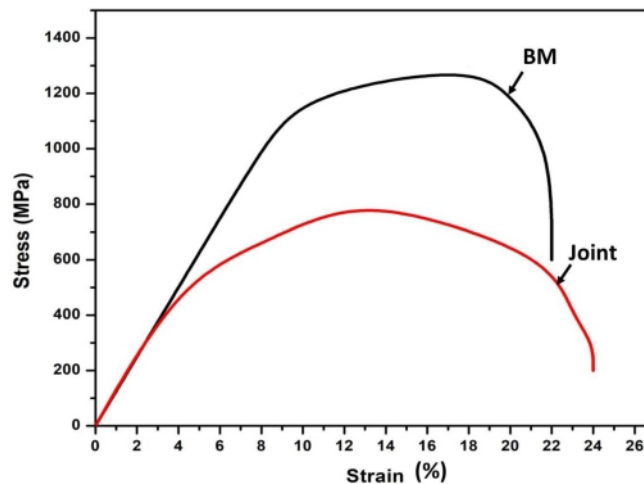
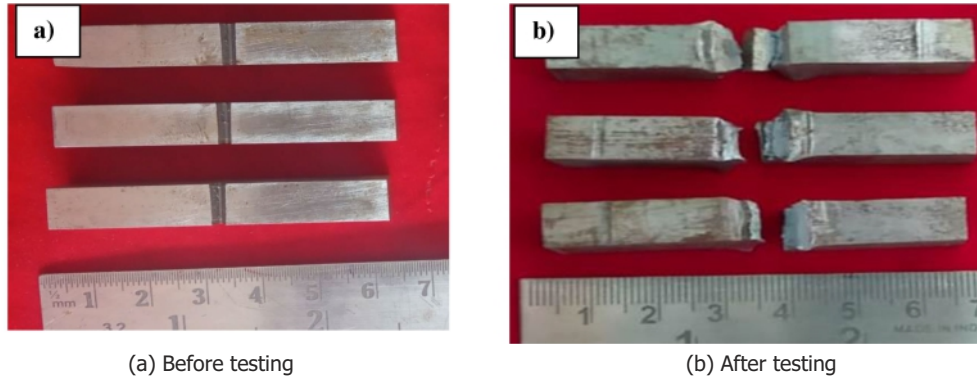


Fig. 7 : Stress – Strain curves of the base metal and welded joint



(a) Before testing

(b) After testing

Fig. 8 : Photographs of impact toughness test specimen

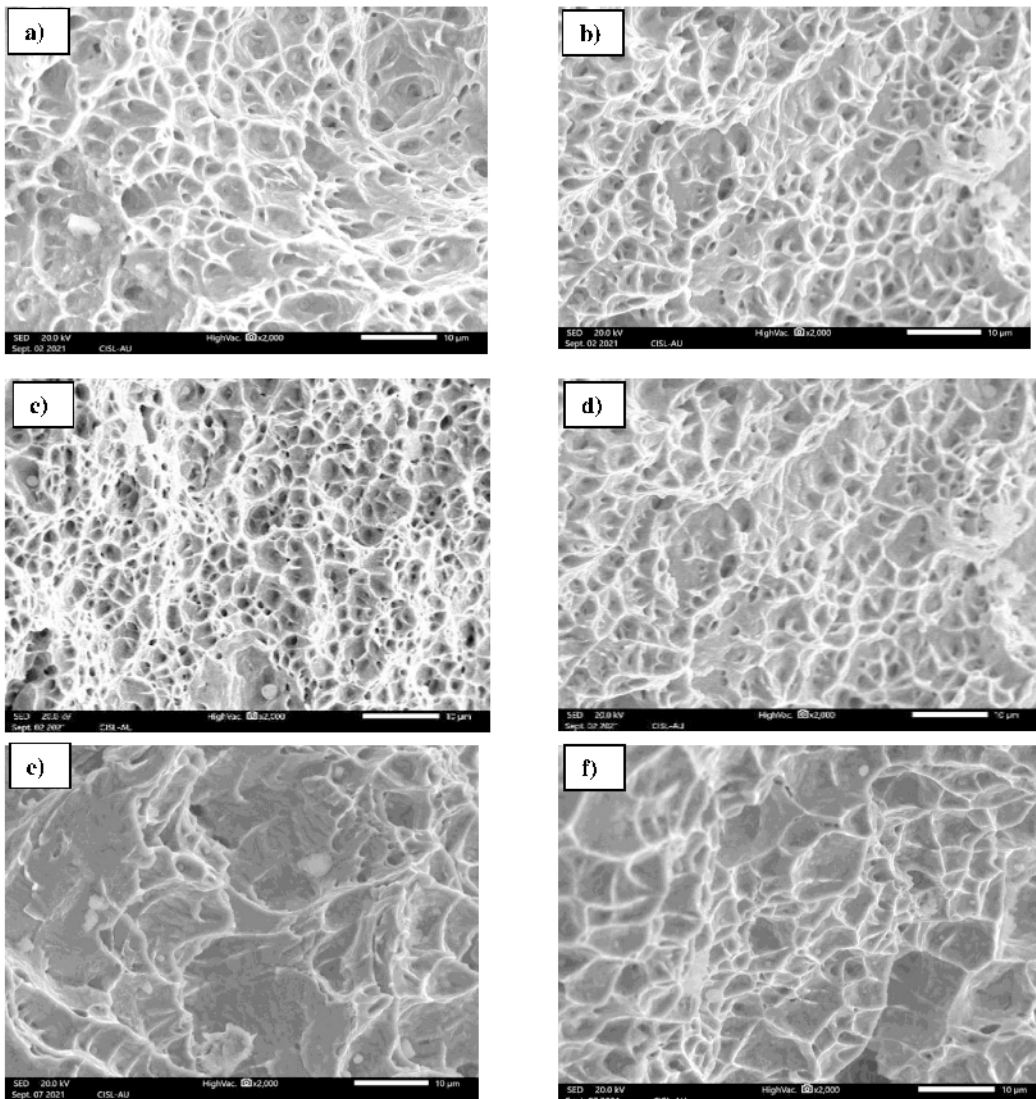


Fig. 9 : Fracture surface of tensile and impact toughness specimens
(a) Base metal (tensile) and (b) Weld Joint (tensile) (c) Base metal (notch tensile) and (d) Weld Joint (notch tensile) (e) Base metal (impact) (f) Weld joint (impact)

3.2 Fractography

The failure region of tested specimens for smooth tensile, notch tensile, and impact toughness was examined using a scanning electron microscope (SEM). **Fig. 9** shows higher magnification SEM pictures of smooth, notch tensile, and impact toughness welded joint specimens. **Fig. 9a** depicts the smooth tensile specimen failure region of BM. It exhibits uniformly distributed fine size dimples. **Fig. 9b** shows smooth tensile failure region of RTA-GMW joint. Failure region exhibits ductile mode of failure and the amount of fine dimples is lower than BM [19]. **Fig. 9c** shows the failure region of a base metal notch tensile specimen. It has a greater number of finer dimples. **Fig. 9d** depicts the notch tensile specimen failure region of the RTA-GMW joint. The volume proportion of fine dimples in this failure region is smaller than in BM. **Fig. 9e** depicts the failure region morphology of a base metal impact toughness specimen. The surface is made up of little dimples. The failure region RTA-GMW joint impact toughness specimen is shown in **Fig. 9f**. The failure region has a ductile mechanism of failure and a greater number of fine dimples than BM [20].

3.3 Microhardness

Fig. 10 illustrates the microhardness among several RTA-GMW joint areas. WM area had the lowest hardness and the BM region had the highest hardness. Unwelded BM has an average hardness of 460 HV; whereas, the WM region of the joint has an average hardness of 321 HV. The WM region of the joint had a 27 % lower hardness than the BM region. The CGHAZ region of the joint has a 9 % lower hardness than the BM zone. The difference in hardness of the WM and HAZ areas is typically due to changes in microstructural properties produced by thermal cycles during welding.

3.4 Metallurgical Behaviour

The cross-sectional optical macrograph pictures of the RTA-GMW joint were displayed in **Fig. 11**. The bead geometry was measured from that macrostructure using Image J analysis software attached to a light optical microscope. As a result (**Table 6**), the WM area of the RTA-GMW joint is calculated to be 90 mm². Further, narrow HAZ width (1.8 mm) has been observed. The BM RHA steel consists of quenched and

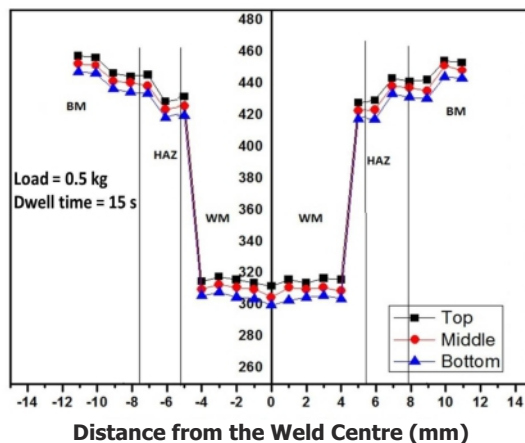


Fig. 10 : Microhardness (HV0.5) variation across the weldment

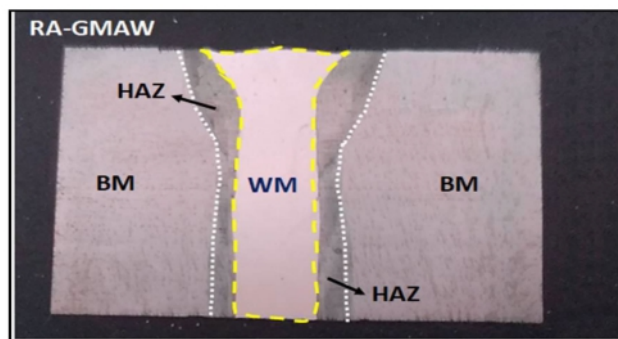


Fig. 11 : Macrostructure of the welded joint

tempered martensite microstructure (as shown in **Fig. 1**). The joint optical micrograph (OM) images of top, middle and bottom regions of WM are shown in **Fig. 12(a-I)**. Microstructure of RTA-GMW joints consists of three distinctive regions such as weld metal (WM) region, fine grain heat affected zone (FGHAZ) region and coarse grain heat affected zone (CGHAZ) region. This distinctive microstructural feature of various regions is formed due to different cooling rate and multi pass welding. The WM mainly consist of delta ferrite (δ -Fe) in a plain austenite matrix. The weld joint microstructure exhibits fine delta ferrite in austenite matrix (**Fig. 12(a-c)**). The WM region volume percentages of delta

Table 5 : Weld bead geometry (macrostructure analysis)

Width of bead (mm)	Depth of penetration (mm)	Weld metal area (mm ²)	HAZ area (mm ²)	Width of the HAZ (mm)	Number of passes	Cumulative heat input (kJ/mm)
7.4	18	90	22.6	1.8	3	2.13

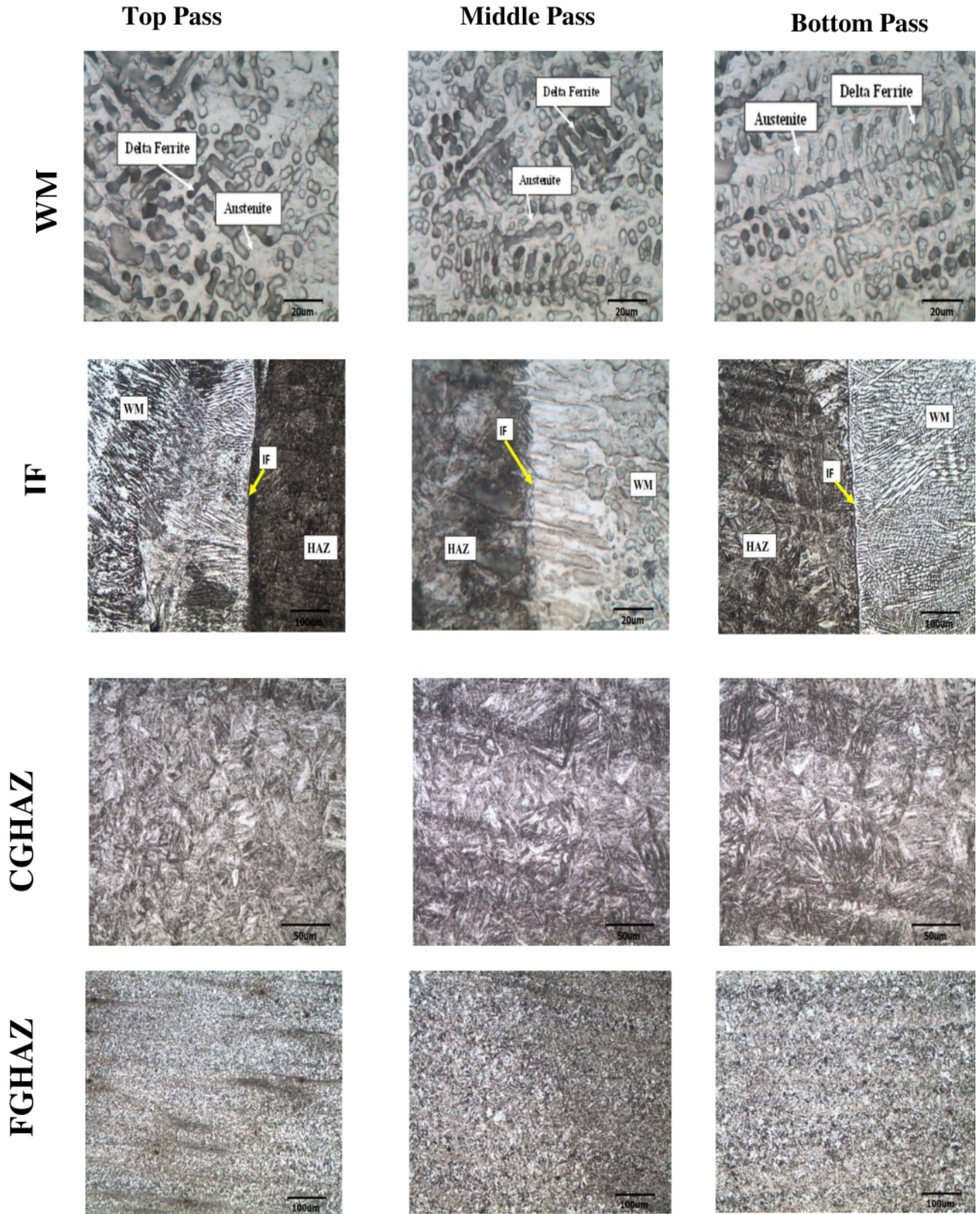


Fig. 12 : Optical micrographs of different regions of weldment

Table 6 : Chemical composition (wt %) of diluted weld metal

C	Si	Mn	P	S	Cr	Mo	Ni	Al	Cu	Ti	V	Fe
0.055	0.070	5.63	0.023	0.018	17.82	0.135	8.36	0.012	0.170	0.002	0.031	Bal

Table 7 : Cr_{eq} / Ni_{eq} ratio of weld metal and Volume fractions of phases (%) in WM

Cr _{eq}	Ni _{eq}	Cr _{eq} / Ni _{eq}	Volume fraction of delta ferrite (%)	Volume fraction of austenite (%)
18.90	8.36	1.53	29.17	70.83

ferrite and austenite are measured by ImageJ analysis software and average results are presented **Table 7**. From that table it is understood that the volume percentage of delta ferrite was 9 % in WM region. **Fig. 12(d-f)** shows interface images of weld joint of top, middle and bottom regions. From that image clearly reveals that the weld joint has very narrow and proper sidewall fusion. **Fig. 12(g-i)** shows the weld joint images of CGHAZ region. The weld joint shows finer martensite structure. **Fig. 12(j-l)** displays the FGHAZ region. This region consists of finer untempered martensite structure. The weight percentage of chemical composition on the diluted WM was determined and is shown in **Table 6**. Weld metal exhibited a significant change in chemical composition when compared to the all-weld metal chemical composition provided by the filler material manufacturer (**Table 1**), owing mostly to the dilution of base metal in weld metal caused by welding. Cr_{eq} and Ni_{eq} of dilute weld metal using the following formulas [21-22] and the results are shown in **Table 7**.

$$Cr_{eq} = Cr \% + Mo \% + 0.7 \times Nb \% \quad (1)$$

$$Ni_{eq} = Ni \% + 35 \times C \% + 20 \times N \% + 0.25 \times Cu \% \quad (2)$$

The Cr_{eq} / Ni_{eq} ratio is calculated using Schaeffler diagram [23] for weld joint and it showed 12 % of delta ferrite in the weld metal region.

4. Discussion

All the weld joint transverse tensile test specimens failed in the weld metal (WM) area, which is attributable to the greater tensile strength of the base metal (1290 MPa). The yield and ultimate tensile strength of the RTA-GMW joint were 784 MPa and 665 MPa, respectively. The yield strength of the weld joint was reduced by 34 % compared to the BM. This is due to higher hardness recorded in base metal region. But when compared

to conventional arc welding (SMAW, GMAW, and FCAW) processes the rotating arc weld joint shows superior transverse tensile strength properties and joint efficiency [24,25]. The strength properties and hardness of WM mainly be governed by on the weld metal microstructure. The WM microhardness is determined by two factors such as, cooling rate and weld metal chemical composition. The different chemical composition of WM produces different microstructure in weld joints. The weld metal region is mostly composed of fine δ -Fe in plain austenite matrix with vermicular δ -Fe morphology. This vermicular δ -Fe morphology has given higher strength and hardness in weld metal [26]. And also, the higher volume percentage of δ -Fe is observed in weld metal region. It has conformed to both ImageJ analysing software and Schaeffler diagram (**Fig. 13**). **Table 6** presents the volume percentage of δ -Fe in the weld joint. This improved volume percentage (12 %) of δ -Fe gives higher strength and hardness in the weld metal. The RTA-GMW processes recorded 2.13 kJ/mm heat input. The rotating arc welding process gives 48 % lower heat input, due to arc rotation reduced heat density at the weld metal (**Fig. 14**), thus arc rotation distributes the heat energy from the weld center, hence weld metal solidified at faster rate. Consequently, the fast-cooling rates drive high volume percentage of fine δ -Fe in the WM area. The chemical composition (wt %) of weld joint are presented in **Table 4**. From that table, it is known that the WM of RTA-GMW joint has contain 8.36 wt.% of Ni element & 19.854 wt.% of Cr element. The RTA-GMW joint has been fine vermicular type δ -Fe in a plain austenitic matrix, it clearly shows important role of nickel in controlling the micro-structure. It significantly increases the WM toughness and strength. As a result, better tensile strength in the rotating arc welding process is reason for creation of a greater volume percentage of delta ferrite and

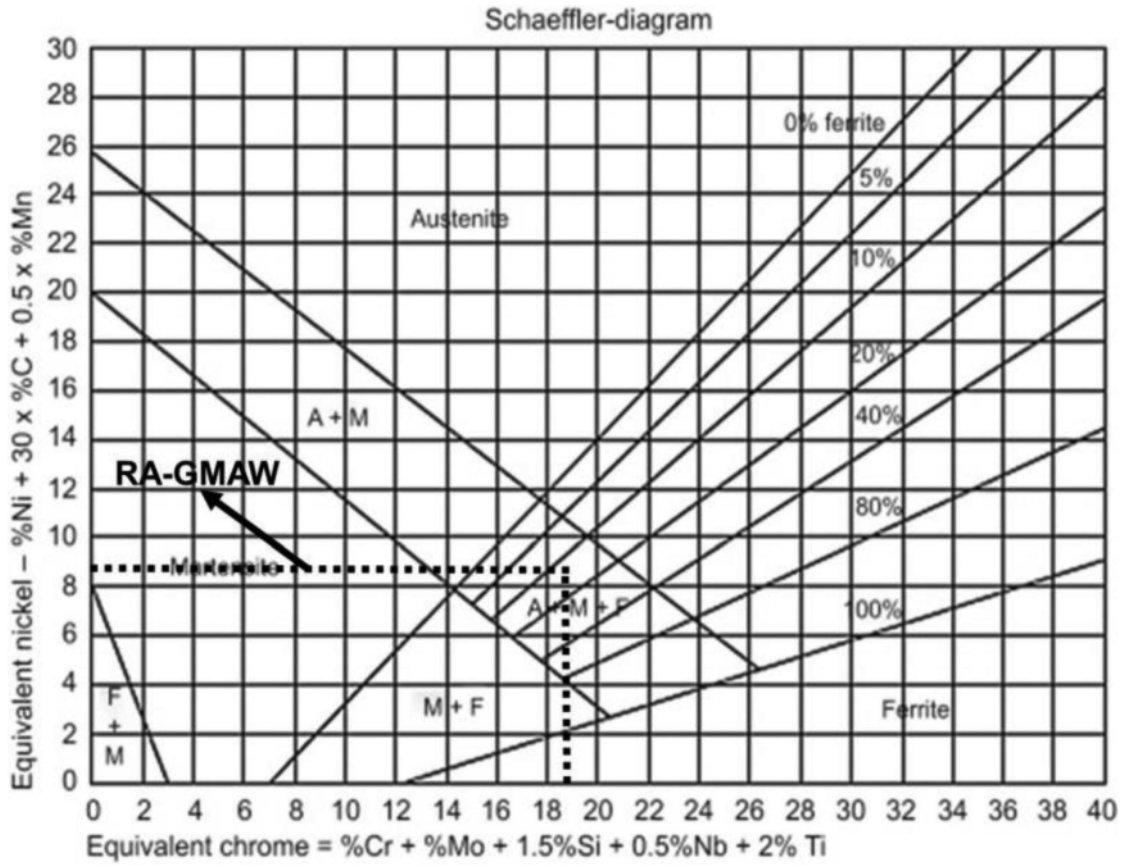


Fig. 13 : Schaeffler diagram

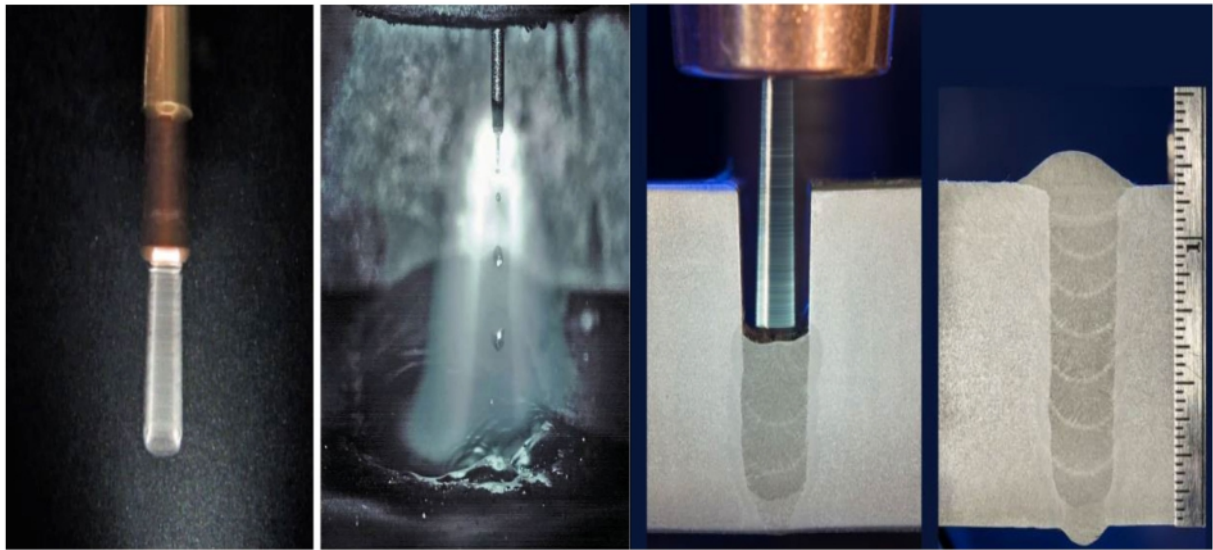


Fig.14 : Rotating arc-welding technology

vermicular δ -Fe morphological structure in the weld metal region. **Table 4** displays the impact toughness values of the BM and weld joint, which are 49 J and 82 J, respectively. The impact toughness of the rotating arc weld joint is 21 % greater than that of the BM. This is due to two major factors: chemical composition of WM and ferrite morphology. This, in turn, is dependent on the cooling rate, and the cooling rate has a direct impact on the solidification mode of WM. The heat input of the welding methods will control this cooling rate. Based on **Table 3**, the heat input of the weld joint was measured to be 2.13 kJ/mm. When compared to regular arc welding methods, the heat input of a RTA-GMW joint is 44 % lower [27]. This is due to high-speed arc rotation (**Fig. 3**), which generates a centrifugal force in the RTA-GMW joint weld metal region. This centrifugal force minimizes the heat density from the weld center and enhances weld joint side wall fusion. Because of the lower heat density in the weld core, the heat input was considerably reduced, and the cooling rate was enhanced to a significant weld joint [28]. For this welding process Cr_{eq}/Ni_{eq} ratio values indicated a ferrite-austenitic (FA) solidification mode. The liquefied weld pool solidified from primary delta ferrite into austenite (γ) in the earlier stages. In general, rotating arc welding method is a low heat input process, so the δ -Fe does not have sufficient time to completely alter into γ . Finally this transformation in vermicular type δ -Fe morphology with γ matrix appears. The calculated delta ferrite content in weld regions is 12 % (according to the Schaeffler diagram). The delta ferrite formed as a constant vermicular network in the γ matrix due to the welding heat input is lower. When the cooling rate is low, there is no time for grain coarsening, hence fine δ -Fe forms in a plain γ matrix with vermicular type δ -Fe morphology in RTA-GMW weld metal. **Table 7** the Ni, Cr and Mg with higher wt.% in RTA-GMW joint weld metal. The increased toughness values of the RA-GMA welded joint is most probably because of the greater amount of chromium in the weld metal area [29]. The occurrence of copper in the WM comes from the BM and the FM and it increases the hardness of the material [30]. Finally, the study determined that the chemical composition of weld metal, higher volume percentage of δ -Fe and vermicular type δ -Fe morphology gives higher impact toughness value in the weld joints.

5. Conclusions

In this work, 18 mm thick rolled homogenous armour (RHA) steel plates were welded by rotating arc GMAW process and the following significant conclusions are derived,

i) The macrostructural analysis confirms that 18 mm thick RHA steel plates can be effectively welded using the rotating arc GMAW technique with full depth of penetration and better sidewall fusion without the formation of any internal or external defects.

- ii) Rotating arc GMAW joints showed greater strength properties such as tensile strength, yield strength, and notch tensile strength than conventional GMAW processes.
- iii) The rotating arc GMAW joint revealed 15 % higher strength properties, 18 % greater weld metal micro-hardness, and 27 % greater impact toughness properties than the conventional GMAW process. This is because the weld metal region contains a greater volume proportion of fine delta ferrite mixed austenitic matrix with vermicular type delta ferrite morphology.

Acknowledgements

The authors would like to express their gratefulness to the Director, CVRDE, DRDO, Avadi, Chennai for funding through CARS project (Project No.CVRDE/18CR0004/MBT/17-18/LP).

Reference

- [1] Magudeeswaran G, Balasubramanian V and Madhusudhan Reddy G M (2008); Effect of welding consumables on tensile and impact properties of shielded metal arc welded high strength, quenched and tempered steel joint, *Sci. Tech. Weld. Joining*, 3(2).
- [2] Balakrishnan M, Balasubramanian V and Reddy G M (2013); Microstructural analysis of ballistic tests on welded armour steel joints, *Met. Mic. Ana*, 2, pp.125–139.
- [3] Magudeeswaran G, Balasubramanian V and Reddy G M (2009); Dynamic fracture toughness (J Id) behavior of armor-grade Q and T steel weldments: Effect of weld metal composition and microstructure, *Met. Mat. Inte.*, 15, pp.1017-1026.
- [4] Madhusudhan R G and Mohandas T (1996); Ballistic performance of high strength low alloy steel weldments, *Jour. Mate. Proc. Tech*, 57, pp.23–38.
- [5] World Pipelines, Magazine (2017); Putting-a-Spin-on-Welding.
- [6] The Article (2017); A new spin on welding GMAW technology improves joining by rotating the wire.
- [7] Sugitani Y and Kobayashi M (1991); Development and application of automatic high-speed rotation arc welding, *Weld. Inte*, 5 (7) 577-583.
- [8] Li W, Gao K, Wu J, Wang J and Ji Y (2015); Groove sidewall penetration modeling for rotating arc narrow gap MAG welding, *Int J Adv Manuf Technol*, 78, pp.573–581.
- [9] Linga Raju D and Raju N (2016); Effect of using a rotating electrode in gas metal arc welding on weld bead characteristics of aluminium alloy 6061-T6 weldments, Vol II, WCE, London, U.K.

- [10] Venkatesh G, Sundararaj P, Verma D K and Arulkumar J (2018) ; Comparison of mechanical and metallurgical properties of conventional GMAW with spin arc GMAW process for carbon steel SA 515, *Int. Res. J.Tech*, 05(05).
- [11] Abo Al Ela M A, Abdo GM, Elmahallawy A M and Sallam M T (2013); Effect of SMAW Welding Parameters on Mechanical and Structure Properties of Welded Joints of the Armoured Steel. *Int. Con. Aero. Scie. Avia. Tech*, pp.1-11.
- [12] Saxena A, Kumaraswamy A, Reddy G M and Madhu V (2018); Influence of welding consumables on tensile and impact properties of multi-pass SMAW ArmoX 500T steel joints vis-a-vis base metal. *Def. Tech.*, 14(3), pp.188-95.
- [13] Amraei M, Ahola A, Afkhami S, Björk T, Heidarpour A and Zhao X L (2019); Effects of heat input on the mechanical properties of butt-welded high and ultra-high strength steels, *Eng. Struc.*, Nov 1,198, 109460.
- [14] Sharma V and Shahi A S (2014); Effect of groove design on mechanical and metallurgical properties of quenched and tempered low alloy abrasion resistant steel welded joints. *Mate. Des.*, 1, 53, pp.727-736.
- [15] Min D, Xin-hua T, Feng-gui L and Shun Y (2014); Welding of quenched and tempered steels with high-spin arc narrow gap MAG system, *Int. J. Adv. Man. Tech.*, 55, pp.527-533.
- [16] ASTM E8-14 (2014); Standard Test Methods for Tension Testing of Metallic Materials.
- [17] ASTM E407-15 (2015); Standard Practice for Micro etching Metals and Alloys.
- [18] Ramaswamy A, Malarvizhi S, Balasubramanian V (2019); Influence of post weld heat treatment on tensile properties of cold metal transfer (CMT) arc welded AA6061-T6 aluminum alloy joints, *J. Mech. Behv. Mate.*, 28, pp.135-145.
- [19] Karthick K, Malarvizhi S, Balasubramanian V, Krishnan S A, Sasikala G and Albert S K (2016); Tensile properties of shielded metal arc welded dissimilar joints of nuclear grade ferritic steel and austenitic stainless steel. *J. Mech. Behv. Mate.*, 25(5-6), pp.171-178.
- [20] Lee J, Kim D, Lee Y C and Lee C (2021); Influence of alloying elements in low temperature transformation Weldment on Ms. temperature, microstructure and mechanical properties, *Mats. Char.*, 171, 110755.
- [21] Balakrishnan M, Balasubramanian V and Reddy G M (2012); Effect of PTA hard-faced interlayer thickness on ballistic performance of shielded metal arc welded armour steel welds, *J. Mat. Engg. Perf*, 22, pp.806-814.
- [22] Naveen Kumar S, Balasubramanian V, Malarvizhi S, Rahman H and A Balaguru V (2021); Influence of welding consumables on ballistic performance of gas metal arc welded ultrahigh hard armour steel joints, *Mats. Perf. Char*, 10(1), pp.443-462.
- [23] Magudeeswaran G, Balasubramanian V and Reddy G M (2018); Metallurgical characteristics of armour steel welded joints used for combat vehicle construction. *Defe. Tech.*, 14, pp.590-606.
- [24] Da Cruz Junior E J, Franzini OD, Calliari I (2019); Effects of nickel addition on the microstructure of laser welded UNS S32750 duplex stainless steel, *Metall. Mater. Trans. A*, 50, pp.1616-1618.
- [25] Goncalves R H, Silva M, Barancell, Schwedersky, Arthur Gustavo Moreira Santos Marcelo Pompermaier (2020); Effects of the rotating arc technique on the GMA welding process, *Technical Papers, Soldag. insp*. 25.
- [26] Dadfar M, Fathi M H, Karimzadeh F, Dadfar M R and Saatchi A (2007); Effect of TIG welding on corrosion behavior of 316L stainless steel, *Matls. Lett.*, 61(11-12), pp.2343-2346.
- [27] Rajani H Z, Torkamani H, Sharbati M, Raygan S (2012); Corrosion resistance improvement in Gas Tungsten Arc Welded 316L stainless steel joints through controlled preheat treatment, *Mate. Des.*, 34, pp.51-57.
- [28] Balaguru V, Balasubramanian V and Shivkumar P (2020); tensile properties of shielded metal arc welded ultrahigh hard armour steel joints, *J Adv Eng Tech Sci.*, 1(2), pp.71-84.
- [29] Saluja R and Moeed K M (2018); Depiction of detrimental metallurgical effects in grade 304 austenitic stainless steel arc welds, *Inter. J. Mech. Pro.*, 8(6), pp.207-218.
- [30] Sriba A, Vogt J B and Amara S E (2018); Microstructure, micro-hardness and impact toughness of welded austenitic stainless steel 316L, *Trans. Ind. Inst. Met.*, 71(9), pp.2303-2314.